Ultrafast Gyroscopic Measurements in a Passive All-Fibre Mach-Zehnder Interferometer via Time-Stretch Technique

Igor Kudelin Srikanth Sugavanam Maria Chernysheva*

Dr. I. Kudelin
Aston Institute of Photonic Technologies, Aston University, B4 7ET, Birmingham, UK
Department of Physics, University of Colorado, 2000 Colorado Ave., Boulder, Colorado 80309, USA
Time and Frequency Division, NIST, 325 Broadway, Boulder, Colorado 80305, USA
Email Address: igor.kudelin@colorado.edu
Dr. S. Sugavanam
School of Computing and Electrical Engineering, IIT Mandi, 175075, Kamand, Himachal Pradesh, India
Dr. M. Chernysheva
Leibniz Institute of Photonic Technology, Albert-Einstein str. 9, 07745, Jena, Germany Email Address: Maria.Chernysheva@leibniz-ipht.de

Keywords: *Fiber-optic Gyroscope; Dispersive Fourier Transformation; Phase; Optical Sagnac Effect; Ultrafast laser*

Almost all inertial navigation systems rely on optical gyroscopes, operating based on the Sagnac effect. Laser gyroscopes allowed High precision measurements in seismology and geodesy. Passive optical gyroscopes, typically fibre-optic gyroscopes (FOGs), are of particular interest due to the lack of a 'lock-in' effect, which is the most detrimental effect in active laser systems. Still, the current data acquisition rate of modern FOGs cannot satisfy emerging applications, particularly for autonomous navigation. Herein, a novel interferometric FOG, based on the measurements of ultrashort pulse phase via the Dispersive Fourier Transformation, is presented, demonstrating the highest up to date acquisition rate of 15 MHz. This passive setup is insensitive to the timing jitter and the fluctuations of the carrier-envelope phase of the incoming pulses. The single-shot resolution of the phase retrieval from the interferometric pattern is 7.3 mrad, which corresponds to a time shift of 8.7 attoseconds. As a confirmation of the high-speed performance, movements of a stepper motor with 300 steps per second have been recorded with an angular velocity resolution of 0.33 mdeg/s with the bias instability of 0.06 deg/h at acquisition time 17.07 μs. The proposed method can facilitate various phase measurements at a high repetition rate and is not limited only by gyroscopic applications.

1 Introduction

Optical gyroscope is an essential tool in inertial navigation and geophysical applications. Their extremely high precision have been proved by accurate measurements of seismic activities [1], the Chandler and annual wobbles of the Earth rotation axis [2]. The operational principle of optical gyroscopes is based on the Sagnac effect [3], which is manifested as a time retardation between counter-propagated beams and leads to a phase shift or offset of oscillation frequencies. Active gyroscopes are based on a laser cavity built in a bidirectional design in order to maintain generation in both counter-propagating directions. Commonly, detection of the Sagnac effect in active laser gyroscopes is based on the measurement of the beat-note frequency, corresponding to the offset of the counter-propagation oscillation frequencies. This method provides the highest resolution but requires sufficient integration time. Moreover, active laser gyroscopes suffer from the so-called 'lock-in' effect at low angular velocities, when the counter-propagating oscillating frequencies are synchronised due to backscattering [4]. This deleterious effect could be eliminated in passive gyroscopes, i. e. interferometers without an active media. Such devices measure the Sagnac effect as a phase shift between counter-propagating pulses. The niche of passive gyros is mostly occupied by fibre-optic gyroscopes (FOGs), since the total sensitivity to the angular motion can be multiplied by coiling the fibre multiple times.
A newly emerged field of gyroscopic measurements is based on exploiting ultrafast lasers [5, 6]. The motivation for using new laser properties is driven by the substantially decreased 'lock-in' effect in ultrafast lasers owing to small spatial interaction length [7]. Moreover, the intensity of the backscaterring light is further reduced due to inherent properties of an intracavity intensity-discriminative saturable absorber, responsible for the mode-locking mechanism. Furthermore, novel data aquisition technique al-

lowed demonstrating a significantly increased acquisition rates up to kHz range, e.g. by analysing real-time spatio-temporal dynamics of ultrashort pulses [8]. A more sophisticated Dispersive Fourier Tranformation (DFT) technique [9] provides single-shot measurements of pulse spectra in MHz rate. Many ultrafast phenomena were experimentally revealed through the DFT measurements, e.g. self-organisation of ultrashort coherent structures [10, 11], spectra pulsations [12] and vibration dynamics of bound solitons [13] to name a few. Moreover, the DFT proved its suitability to characterise phase stability of the ultrashort pulse train [14] and other practical applications as an all-optical digitiser [15], imaging [16], displacing sensing [17] and LiDAR systems [18].
The DFT measurements of counter-propagating pulse in bidirectional fibre lasers demonstrated their complex dynamics of soliton collisions, energy exchanges, and central wavelength drifts and synchronisation with tendency to Q-switched instability or multi-soliton operation [19, 20, 21]. Such dynamics is particularly detrimental for gyroscopic measurements. Thus, previous works on ultrafast laser gyroscopes indicated that the resolution is strongly limited by the stability of the carrier-envelope phase (CEP) [6, 8]. Overall, bidirectional laser systems inherit more sophisticated cavity design and require subtle adjustment to achieve efficient stabilisation of the mode-locking operation regime.
In this work we propose a combination of advantages of passive fibre optic gyroscopes with the benefits of ultrashort pulse operation regime and real-time measurements. The demonstrated simple concept is based on a unidirectional mode-locked fibre laser and a Mach-Zehnder interferometer (MZI), placed on the rotation platform. With the transit to unidirectional lasers we ensure the efficient stabilisation of the pulsed generation at the high level that is inaccessible for bidirectional mode-locked lasers, used in active gyroscopes. Since the Sagnac effect is measured through phase shift in passive gyroscopes, the combination of the DFT interferometry and ultrashort pulses opens the opportunities to simultaneously achieve both high data acquisition rate and measurements precision, thus, substantially outperform small-sized active gyroscopes. While propagating at two separate arms of the MZI, a complex collision dynamics between the counter-propagated solitons is completely avoided. Moreover, the MZI design ensures the interfere of the pulse with itself. This helps eliminating the problem of the carrier-envelope phase stability, since and the phase fluctuations of the incoming pulses are cancelled out. Furthermore, the setup is insensitive to the timing jitter. The achieved in this work data rate of the gyroscopic measurement is $\tilde{1}5$ MHz, which is limited by the repetition rate of the used mode-locked fibre laser. The results of this work demonstrate the single-shot resolution of the phase retrieval of 7.2 mrad that corresponds to a timing shift of 8.6 as and angular velocity of $\sim$0.33 mdeg/s. The bias instability, which is the lowest value of the Allan deviation, of 0.06 deg/h is achieved at the integration time of 17.07 μs. We have confirmed the acquired phase measurements with extracted a time separation between the pulses, that is encoded in the interferometric pattern. Finaly, we have also demonstrated that this setup can measure angular acceleration with single-shot resolution of 4.98 kdeg/s^2. We believe that this work provides a new insight on phase-based measurements at high acquisition rates and is not limited to only gyroscopic applications.

2 Results and discussion

The demonstrated system is based on Mach–Zehnder interferometer which splits the pulse into two equal replicas via 3-dB fibre coupler. The nearly equal length of each arm of the interferometer ensures that the pulse interferes with itself. Numerically, during the rotation of the MZI the phase of the pulse in each of the arms can be expressed as $\phi_1 = \delta\phi + \phi_{delay1} + \phi_{Sagnac}$ and $\phi_2 = \delta\phi + \phi_{delay2} - \phi_{Sagnac}$. Here $\delta\phi$ is the phase of the pulse at the input of the MZI, ϕ_{delay1} and ϕ_{delay2} are the accumulated phases in the different arms of the interferometer. The sign of ϕ_{Sagnac}, which is the phase shift associated with the Sagnac effect, depends on the direction of the angular rotation. Therefore, the resulting relative phase is the difference between the phase of each pulse $\Delta\phi = \phi_1 - \phi_2 = \phi_{delay1} - \phi_{delay2} + 2\phi_{Sagnac} = \Delta\phi_{delay} + 2\phi_{Sagnac}$, which makes Sagnac-induced phase shift independent to the phase fluctuations of the incoming pulses. Note, in case if only one arm of the interferometer is placed on the rotation platform, the Sagnac phase response will not be multiplied by a factor of two. The phase component $\Delta\phi_{delay}$ is responsible

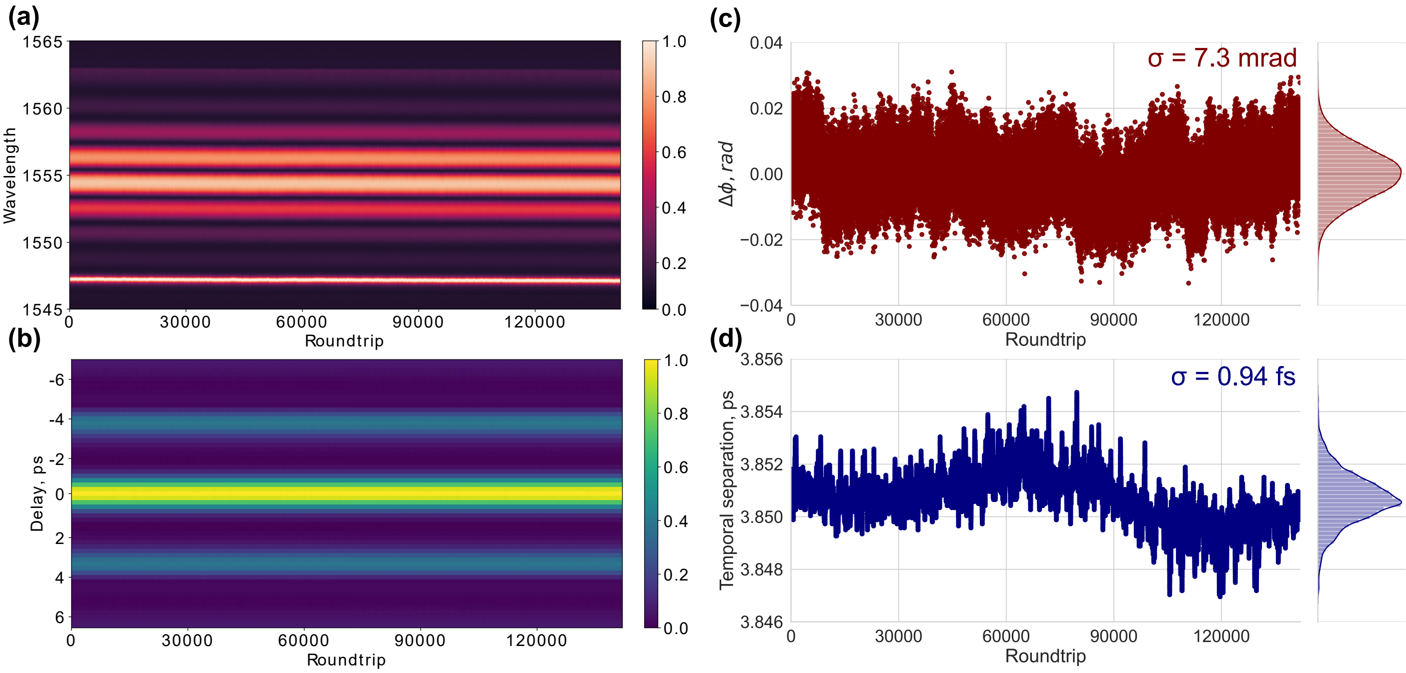

Figure 1: **(a)** The DFT measured spectra from the Mach-Zehnder-interferometer at rest. **(b)** The single-shot first-order autocorrelation function, numerically obtained from the DFT spectra. **(c)** The single-shot extracted relative phase with corresponding probability density function. The standard deviation is 7.3 mrad. **(d)** Temporal separation between the pulses with moving averaging window of 100 roundtrips.

for the difference between the lengths of both arms of the interferometers and, ideally, remains constant over time. But, since the optical path can fluctuate over time, e.g. due to temperature fluctuations, this phase term presents the main source of error uncertainty of the measurements.

Figure 1(a) demonstrates the recorded DFT spectra of the pulses interference when the gyroscope platform is at rest. The corresponding roundtrip-resolved first-order autocorrelation is shown in Figure 1(b). The figures clearly indicate a stable interference between two pulses with high modulation depth. Figure 1(c) shows the extracted relative phase from the interferometric pattern with the corresponding probability density function, using the algorithms described in [13, 14]. The standard deviation is 7.3 mrad that corresponds to 8.7 as timing shift at central wavelength of 1555 nm. The standard deviation defines the smallest distinguishable relative phase change from noise that equals to the resolution of the proposed phase method. Due to the normal distribution, the standard deviation, and the minimum resolution as a consecutive, could be further enhanced by $\sqrt{n}$ by averaging over n roundtrips, obeying the normal distribution for a white noise. However, the averaging will come at a price of a decreased acquisition rate by n times.

Figure 1(d) demonstrates the relative timing separation between the pulses from the interferometer with a moving averaging window of 100 round trips, resulting in the temporal resolution of 0.78 fs. The average temporal separation is 3.85 ps with a standard deviation of 0.94 fs. A low value of the standard deviation evidences that the measurements of the relative phase are not affected by the timing jitter of the laser source. Indeed, the timing jitter is converted into a temporal fluctuation of the arriving time of the pulse to the interferometer input. The reduced sensitivity to the fluctuations of the incoming pulses has been confirmed in our previous studies, utilising similar measurements approach [14]. Nevertheless, due to the time-frequency duality of the DFT measurements, the timing jitter can introduce uncertainties of the central wavelength in the interferometric pattern, converting to the fluctuations of the relative phase. But this effect is significantly reduced, compared to the unidirectional lasers, where timing jitter is directly converted to the phase fluctuations.

The timing jitter of the laser source can affect the measurements of the platform acceleration, but its effect could be neglected since the timing jitter is is sufficiently lower compared to the round trip time period. The uncertainty of the angular acceleration measurements due to the timing jitter of the laser

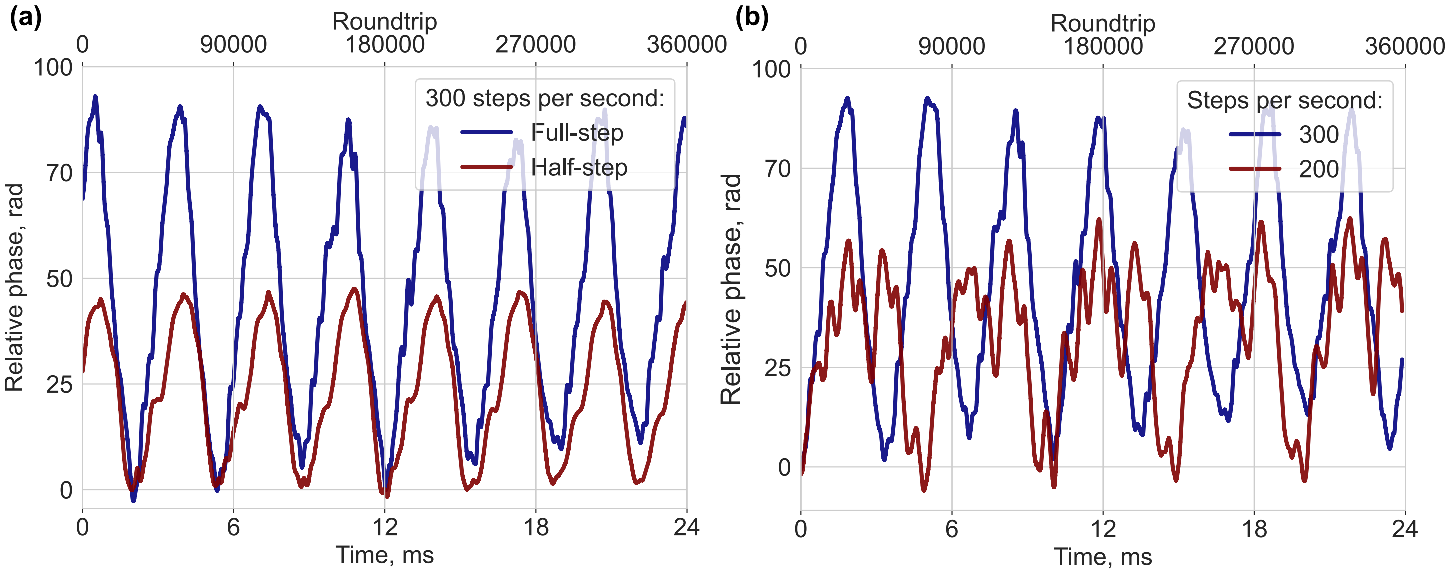

Figure 2: (**a**) Relative phase dynamics under rotational exposure by a stepper motor with full-step (blue line) and half-step size (red line) at 300 steps per second (50 000 roundtrips or 3.33 ms per step). (**b**) Relative phase dynamics under rotational exposure by a stepper motor, set to produce 300 steps per second (blue line) and 200 steps per second (75 000 roundtrips or 5 ms per step; red line) at full-step size.

source can be estimated as $\Omega_{jitter} = \tau_{jitter}/T_{rep}$, where Ω_{jitter} is the uncertainty in the measurements of the angular acceleration due to the timing jitter, τ_{jitter} is the timing jitter and T_{rep} is the pulse timing period.

We have verified the capabilities of the proposed real-time measurement technique by capturing the phase dynamic while rotating the MZI using a stepper motor with an adjustable step size and angular velocity (steps per second). The stepper motor presents a conventional test-bed for investigating the response of the measurements setup particularly to dynamically varying angular velocities. The full step size of the stepper motor produces an angular shift of the gyroscopic platform of 7.1 mdeg (124.6 μrad). The stepper motor was set to angular velocity of 300 steps per second, corresponding to one step duration of 3.3 ms or 50 000 roundtrips of used ultrafast fibre laser. **Figure 2** demonstrate the gyroscopic measurements with full and half step sizes, which corresponds to the average platform angular velocity of 2.13 deg/s (0.037 rad/s) and 1.07 deg/s (0.0186 rad/s), correspondingly. The angular rotations produced the average phase shift of 47.22 rad and 23.08 rad, respectively. The recorded step duration is in a good agreement with the anticipated value of 3.3 ms per step. Moreover, the Figure 2(a) clearly shows the decrease in phase shift when the stepper motor operates in the half-step regime.

Figure 2(b) compares the phase measurements at different speeds of the stepper motor. The motor was set to produce 300 steps per second and 200 full steps per second (step duration of 75 000 roundtrips or 5 ms). The obtained average shift at 200 full steps per second is 32.73 rad. The observations provide a good temporal agreement between the set temporal duration of the step and the observed duration of the motor step cycle. The motor step at the setting of 200 steps per second starts to experience a complex two-peak angular profile due to a longer switch between the coils of the stepper motor. As expected, the presented passive gyroscope configuration does not have any synchronisation dynamics or lock-in effect. These observations confirm that ultrashort pulses could be effectively used for gyroscopic measurement in a passive configuration.

Comparison of the data on the relative phase and the relative temporal position between the pulses at the output of the interferometer, extracted from the same interferometric pattern, is shown in **Figure 3(a)**. To plot the relative phase in the time domain we transformed the phase data by using the phase-time relation $\phi = t \cdot \omega$, where ω is the carrier angular frequency of the pulse. The single-shot resolution of the temporal measurements is 7.8 fs. The average temporal shift is 39.82 fs, corresponding to a error with the phase data of only 4%. Such a good agreement between both measurements supports our results on gyroscopic measurements. Furthermore, both data of relative phase data and temporal measurements

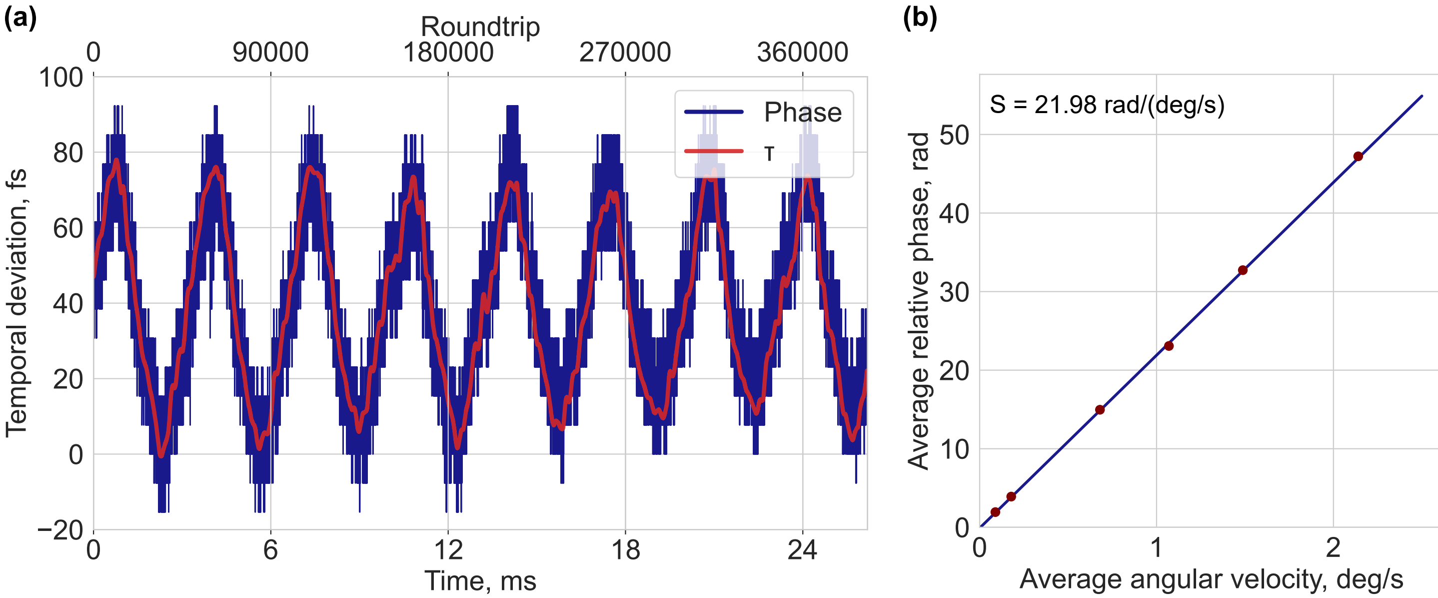

Figure 3: (**a**) Dynamics of the relative phase (red line) and the relative temporal separation (blue line) between the pulses from the interferometer extracted from the same interferometric pattern. The phase data was converted to the temporal domain by using the phase-time relation. The motor was set to produce 300 steps per second at full-step size (50 000 roundtrips or 3.33 ms per step). (**b**) The experimentally obtained relation between applied average angular velocity and the observed average shift in relative phase with linear approximation. The resulting scale factor is 21.98 rad/(deg/s).

can be further simultaneously used to increase the total resolution of the setup.

The scale factor of the passive gyroscope configuration was estimated from a linear approximation between the applied average angular velocity and the observed average shift of the relative phase and depicted in Fig. 3(b). The applied angular rotation was ranging from 89.3 mdeg/s (200 steps per second at 1/16 step size) up to 2.14 deg/s (300 full steps per second). The resulting scale factor is 21.98 rad/(deg/s) or 18.02 fs/(deg/s).

Here, we would like to note that the experimentally obtained scale factor is significantly exceed the theoretical value based on the Sagnac equations. To investigate that observations, we implemented a few different setups, including (i) interferometer with normal dispersion fibre arms; (ii) the DFT coil positioned before and after the interferometer; and (iii) the DFT spool with different values of the GVD. All of the discussed configurations demonstrate the same scale factor. In previous works it have been demonstrated that laser gyroscopes can experience significantly increased Sagnac effect due to nonlinearly induced non-reciprocity [22], dispersion [23, 24] or by operating near exceptional points [25, 26].

The maximum detectable angular velocity is limited by the range of inter-pulse temporal separation while the interferometric pattern is preserved. This temporal range is estimated to ∼340 ps [14]. To allow the gyroscope operate in both directions, this value should be halved to estimate the maximum measurable angular velocity. For the experimentally obtained scale factor of 18.02 fs/(deg/s), the maximum velocity is limited by 9.43 kdeg/s. The maximum observable angular velocity could be further increased proportionally to the spectral resolution of the DFT.

The measurement limitations are also applied for the measurements of the maximum angular acceleration of the platform. The acceleration of the platform could be calculated by differentiation of the data on angular velocity over roundtrips and plotted in **Figure 4**. The single-shot resolution of the acceleration is defined as the standard deviation divided by the time period of the pulse train and constitutes 4.98 kdeg/s^2. However, to resolve the acceleration of the stepper motor we used a moving averaging window over 1 000 roundtrips which provide the resolution of ∼5 deg/s^2. The theoretical average acceleration during the first half of the step cycle is 2571.4 deg/s^2 while the experimentally obtained value is 2253.5 deg/s^2. The error between these two results is mostly due to the step profile of the stepper motor, which is different from the sine approximation. This can be seen from Fig. 4, that the step cycle has the acceleration with a positive sign of longer time duration than the half of the cycle and longer than

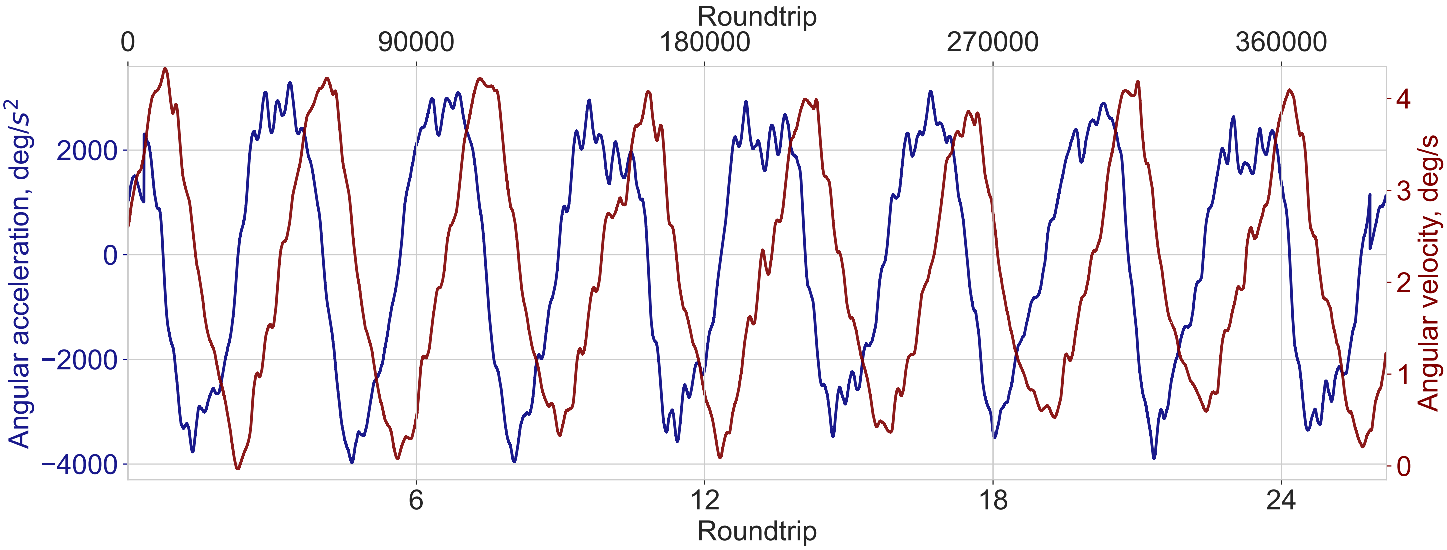

Figure 4: Angular acceleration (blue line) and angular velocity (red line) of the laser platform during rotation exposure by the stepper motor. The motor was set to produce 300 full steps per second (50 000 roundtrips or 3.33 ms per step). The acceleration was obtained by differentiating the velocity over a window of 10 000 roundtrips to increase the resolution.

a further deceleration of the platform. The resulting average acceleration per step is -12.7013 deg/s^2, which is close to zero with a residual mistake of around 0.56% related to the mean value of acceleration. The measurements of angular acceleration are significant as they provide more information about the dynamics of the platform.

The maximum applied angular acceleration is restricted due to the periodicity nature of the interferometric pattern, so the total Sagnac phase shift should not exceed π per each pulse. Hence, the maximum angular acceleration, that could be unambiguously retrieved, is determined as the angular velocity corresponded to the phase shift of π divided by the pulse period and is equal to 2.14 Mdeg/s^2. As in active gyroscopes, the maximum angular acceleration could be increased by using the laser with a higher repetition rate. However, contrary to active systems, the presented approach will not affect the resolution of the angular velocity measurements in a passive gyroscope configuration. Moreover, the higher repetition rate of the ultrafast laser source will also result in a higher data frequency of the gyroscopic measurements. Thus, for more precise measurements of the angular acceleration, laser sources with a lower timing period between pulses are preferred.

Finally, we assessed the performance of the proposed passive gyroscope for measurements of angular velocities. The angular velocity resolution in the single-shot regime is estimated to be 0.33 mdeg/s (5.8 μrad/s), based on the scale factor of 21.98 rad/(deg/s) and the standard deviation of the reference measurements of 7.3 mrad. For the full description of the gyroscope performance, we calculated the Allan deviation of the retrieved phase and demonstrate it in **Figure 5**. The Allan deviation is a traditional approach to estimate noise and stability of oscillating frequency over different time scales and is widely used in clock systems, gyroscopes, and other applications where high stability is required [27]. The maximum integration time of 8.7 ms is limited by the memory of the oscilloscope. The calculated Allan deviation shows two strong trends, which are related to the noises of the system. The Allan deviation is decreasing with $1/\sqrt{t}$ trend, which is related to the averaging of the white noise. The minimum Allan deviation of 0.06 deg/h (0.29 μrad/s) is observed at the integration time of 17.07 μs. So, the maximum resolution could be achieved at the data rate of 58.6 kHz. At the integration time longer than 17 μs the Allan deviation start to increase with a rate of $\sqrt{t}$ due to long-term uncompensated noises.

Such a low value of the bias instability presents a significant improvement when compared to previous results [5] and is close to meet the requirements for laser gyros used for navigation purposes [28, 29]. Additionally, the demonstrated here passive gyroscope is able to provide measurements at data rate by orders of magnitude higher than even the fastest commercially available instruments and is limited by the speed of light. Furthermore, since the accumulated Sagnac phase shift depends on the covered area

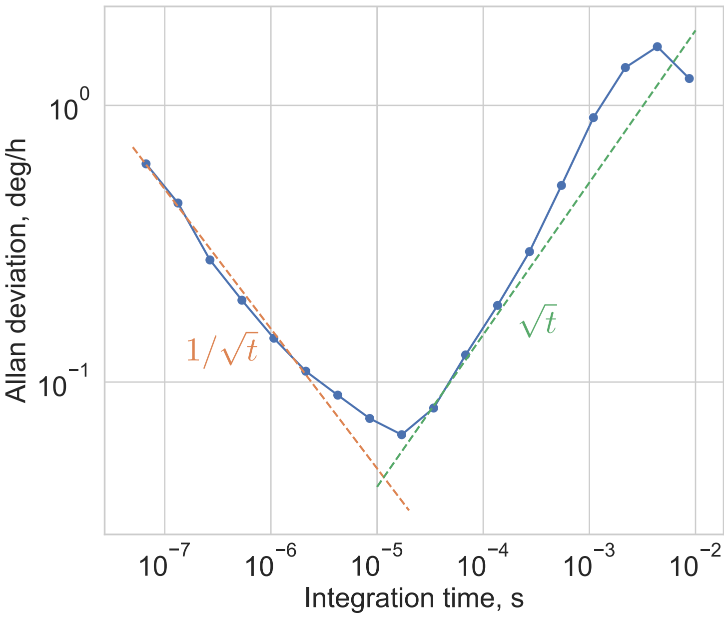

Figure 5: Allan deviation of the relative phase dynamics in a passive gyroscope during the reference measurements.

as $A = \frac{L \cdot R}{2}$, where R is the radius of the covered circular area, the resolution can be improved by increasing the radius of the gyroscope.

3 Conclusion

In this work we demonstrated gyroscopic measurements in the passive all-fibre setup, based on MZI and ultrafast fibre laser. The Sagnac phase shift was retrieved through the DFT interferometry at a data rate of 15 MHz. The extracted phase data was confirmed by the simultaneous deriving of the temporal inter-pulse separation. The single-shot resolution of the phase was 7.3 mrad, which corresponds to the single-shot resolution of the angular velocity of 0.33 mdeg/s with the scale factor of 21.98 rad/(deg/s). The scale factor was obtained by measuring the average phase shift at various angular velocities in the range from 89.3 mdeg/s to 2.14 deg/s. We would like to note, that the obtained scale factor significantly exceeds the theoretical value, based on the classical Sagnac equations. The maximum measurable angular velocity is 9.43 kdeg/s, limited by the spectral resolution of the DFT measurements. The bias instability, assessed as a minimum value of the Allan deviation, was 0.06 deg/h at the integration time of 17.07 μs (58.6 kHz). Finally, we presented the measurements of the angular acceleration of the rotation platform with the single-shot resolution of 4.98 Mdeg/s^2, which could be further decreased, inversely proportional to the number of the integrated roundtrips. The maximum angular acceleration of the current gyroscope operation is 2.14 Mdeg/s^2.

The proposed passive gyroscopes possesses several advantages compared to the previous works utilising similar measurement techniques or employing ultrafast laser systems. First, passive gyroscope requires a unidirectional mode-locked laser, which presents the more mature technology compared to the bidirectional mode-locked lasers, and, therefore, features higher stability and less complicated pulse dynamics. Moreover, the passive configuration of MZI allows overcoming one of the main limitations of active ultrafast laser gyroscopes, i.e. dependency on temporal and phase fluctuations of ultrashort pulses. Our results also experimentally confirmed that the MZI gyroscopic measurements are not affected by such kind of laser instabilities, which essentially relaxes the requirements set on the seed source performance. Furthermore, the demonstrated setup is free of the 'lock-in' effect or collision dynamics between the counter-propagating pulses.

While the reported for the first time in this work the MZI-based gyroscope combined with analysis of real-time ultrashort pulse dynamics has demonstrated excellent capability, the overall gyroscope performance could be further enhanced. While the influence of the instabilities of the laser source are signif-

icantly reduced, further stabilisation would reduce the residual fluctuations and increase the gyroscope performance at longer integration time. For example, the Allan deviation and the resolution of the angular rotation can be improved by providing active and passive stabilisation of both the laser source and the arms of the interferometer. The performance of the proposed gyroscope can be also boosted by using polarisation-maintaining fibre, which is commonly used in passive optics gyroscopes. Moreover, a temperature-insensitive interferometer, shown in Ref. [30], can substantially decrease the influence of the temperature fluctuations and provide lower values of the Allan deviation over the long time scales.
All in all, the proposed setup can operate at a broad range of applied angular velocity and acceleration. The usage of the DFT interferometry for phase measurements configuration demonstrated itself as a perfect combination for precision gyroscopic measurements at high data rates. Nevertheless, the presented concept of the DFT interferometry could be extended to other phase-based applications and is not limited by the gyroscopic measurements.

4 Experimental Section

Figure 6 demonstrates the experimental setup of the used mode-locked fibre laser associated with the Mach-Zehnder interferometer, positioned on rotation platform for measurements of the angular velocity. The stable generation of ultrashort pulses was achieved by using hybrid mode-locking, i.e. the co-action of single-walled carbon nanotube saturable absorber and the modulator based on the nonlinear polarisation rotation (NPE). The latter one was realised by insertion of a section of polarising fibre (HB1550Z from Thorlabs) and a pair of polarisation controllers. While the laser cavity lacked an optical isolator, the unidirectional generation with more than 20 dB extinction ratio has been ensured by proper adjusting the polarisation controllers. As the result, the laser generates 570-fs pulses with the average output power of 1 mW and time-bandwidth product of 0.35 in the clockwise direction at a 15-MHz repetition rate. More details on the laser can be found in Ref. [31]. The DFT line consists of an 11 km of dispersion compensating fibre (WBDK-70-L from OFS) with a total group velocity dispersion D = -1200 ps/nm at 1555 nm. The optical signal is recorded by a 50-GHz photodiode (Finisar XPDV2320R) and a 33-GHz 80-GSa/s digital storage oscilloscope (Agilent DSOX93204A). The spectral resolution of the DFT measurement, limited by the bandwidth of the used photodiode and the oscilloscope, is 0.021 nm [9].
The Mach–Zehnder interferometer consist of two 3-dB fibre couplers with almost equal arms. The total length of each arm of the interferometer is 12.7 m. A negligible difference between the lengths of both arms of $\tilde{5}$ mm is introduced in order to achieve the interferometric pattern. The length of the interferometer has to be close to the length of the laser cavity so that only one pulse is circulating inside the interferometer. This aspect is important to acquire unique and unambiguous data on the Sagnac effect from the interferometer. Should the length of the interferometer arms be different from the laser cavity

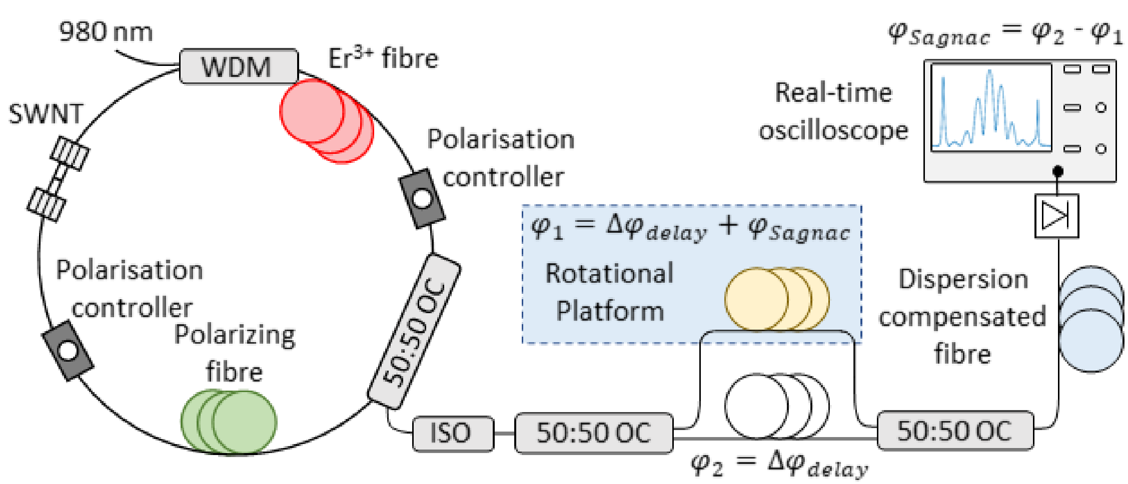

Figure 6: The measurement setup.

roundtrip, the measurement pattern would not be periodic leading to multi-value data or the absence of the rotation data. To minimise further the effect of the temperature fluctuations on the length of MZI arms, they were covered with a foam box.

Data Availability Statement
The data that support the findings of this study are openly available in figshare at http://doi.org/10.6084/m9.figshare.19430615, reference number 19430615.

References

[1] A. Pancha, T. Webb, G. Stedman, D. McLeod, K. Schreiber, *Geophysical Research Letters* **2000**, *27*, 21 3553.

[2] K. U. Schreiber, T. Klügel, J.-P. R. Wells, R. B. Hurst, A. Gebauer, *Physical Review Letters* **2011**, *107* 173904.

[3] G. Sagnac, *Comptes Rendus* **1913**.

[4] F. Aronowitz, R. Collins, *Applied Physics Letters* **1966**, *9*, 1 55.

[5] I. Kudelin, S. Sugavanam, M. Chernysheva, *Sensors* **2021**, *21*, 10 3530.

[6] A. A. Krylov, D. S. Chernykh, E. D. Obraztsova, *Optics Letters* **2017**, *42*, 13 2439.

[7] J. Chesnoy, *Optics Letters* **1989**, *14*, 18 990.

[8] M. Chernysheva, S. Sugavanam, S. Turitsyn, *APL Photonics* **2020**, *5*, 1 016104.

[9] K. Goda, B. Jalali, *Nature Photonics* **2013**, *7*, 2 102.

[10] G. Herink, B. Jalali, C. Ropers, D. Solli, *Nature Photonics* **2016**, *10*, 5 321.

[11] J. Peng, M. Sorokina, S. Sugavanam, N. Tarasov, D. V. Churkin, S. K. Turitsyn, H. Zeng, *Communications Physics* **2018**, *1*, 1 20.

[12] M. Liu, Z.-W. Wei, H. Li, T.-J. Li, A.-P. Luo, W.-C. Xu, Z.-C. Luo, *Laser & Photonics Reviews* **2020**, *14*, 4 1900317.

[13] Z. Wang, K. Nithyanandan, A. Coillet, P. Tchofo-Dinda, P. Grelu, *Nature Communications* **2019**, *10*, 1 830.

[14] I. Kudelin, S. Sugavanam, M. Chernysheva, *Optics Express* **2021**, *29*, 12 18734.

[15] A. Fard, B. Buckley, S. Zlatanovic, C.-S. Bres, S. Radic, B. Jalali, *Applied Physics Letters* **2012**, *101*, 5 051113.

[16] K. Goda, A. Ayazi, D. R. Gossett, J. Sadasivam, C. K. Lonappan, E. Sollier, A. M. Fard, S. C. Hur, J. Adam, C. Murray, C. Wang, N. Brackbill, D. Di Carlo, B. Jalali, *Proceedings of the National Academy of Sciences* **2012**, *109*, 29 11630.

[17] K. Goda, K. K. Tsia, B. Jalali, *Applied Physics Letters* **2008**, *93*, 13 131109.

[18] Y. Jiang, S. Karpf, B. Jalali, *Nature Photonics* **2020**, *14*, 1 14.

[19] I. Kudelin, S. Sugavanam, M. Chernysheva, *Photon. Res.* **2020**, *8*, 6 776.

[20] I. Kudelin, S. Sugavanam, M. Chernysheva, *Communications Physics* **2020**, *3*, 1 1.

[21] Z. Wang, Q. Jiang, Z. Tang, Z. Zhang, *Optics Express* **2020**, *28*, 19 28209.

[22] A. Kaplan, P. Meystre, *Optics Letters* **1981**, *6*, 12 590.

[23] J. Hendrie, M. Lenzner, H. Afkhamiardakani, J. C. Diels, L. Arissian, *Optics Express* **2016**, *24*, 26 30402.

[24] D. D. Smith, H. Chang, L. Arissian, J. C. Diels, *Physical Review A* **2008**, *78* 053824.

[25] Y.-H. Lai, Y.-K. Lu, M.-G. Suh, Z. Yuan, K. Vahala, *Nature* **2019**, *576*, 7785 65.

[26] S. Sunada, *Physical Review A* **2017**, *96*, 3 033842.

[27] O. J. Woodman, An introduction to inertial navigation, Technical report, University of Cambridge, Computer Laboratory, **2007**.

[28] W. Chow, J. Gea-Banacloche, L. Pedrotti, V. Sanders, W. Schleich, M. Scully, *Reviews of Modern Physics* **1985**, *57*, 1 61.

[29] A. Braga, J.-C. Diels, R. Jain, R. Kay, L. Wang, *Optics Letters* **2010**, *35*, 15 2648.

[30] W. Zhu, E. R. N. Fokoua, Y. Chen, T. Bradley, M. N. Petrovich, F. Poletti, M. Zhao, D. J. Richardson, R. Slavík, *Optics Letters* **2019**, *44*, 11 2768.

[31] M. Chernysheva, M. Al Araimi, H. Kbashi, R. Arif, S. V. Sergeyev, A. Rozhin, *Optics Express* **2016**, *24*, 14 15721.